Methyl Tunnelling and Reorientation in the Solid Tetramethyl Compounds of Silicon, Germanium Tin and Lead, and in Methyl Lithium

W. Müller-Warmuth, K.-H. Duprée

Institut für Physikalische Chemie der Universität Münster, Münster

M. Prager

Institut für Festkörperforschung der KFA Jülich

Z. Naturforsch. **39 a**, 66–79 (1984); received October 17, 1983

Quantum-mechanical tunnelling and thermally activated reorientation of methyl groups have been studied in the series compounds $X(CH_3)_4$ with X = Si, Ge, Sn, Pb and $LiCH_3$ using NMR and, if possible, neutron scattering (INS and QNS) techniques. The temperature and frequency dependence of the relaxation rates $1/T_1$ and $1/T_{1\varrho}$ mirror the transition from small to large tunnel splittings as the barrier to rotation decreases in the succession X = Si, $LiCH_3$, X = Ge, Sn, Pb. The various relaxation maxima, correlation times and apparent activation energies have been discussed in terms of current theories. Using the NMR, INS, QNS results and available literature data, relationships between tunnelling and temperature, activation, molecular structure and potential functions have been derived. Potential barriers decrease from about 7 to 0.2 kJ/mol and the symmetry is not far from threefold.

1. Introduction

Rotational tunnelling of methyl groups in solids has recently received much attention. CH_3 groups may perform one-dimensional rotations about their threefold axes hindered by a potential barrier which has its origin in the interaction with neighbouring atoms and molecules. Studying such type of hindered rotation provides an excellent and simple example for a better understanding of transport processes in general, where, owing to temperature effects, the two limits of quantum motion and thermally activated random reorientation can both be realized. At low temperatures, tunnelling manifests itself as a splitting of the torsional ground state. This splitting can be directly observed by inelastic neutron scattering (INS) [1] and it affects nuclear magnetic resonance (NMR) experiments in a characteristic manner [2–7]. In the high temperature limit, on the other hand, the rotation can be treated classically and barrier heights as well as thermally activated reorientation rates have been measured for many years using NMR spin-lattice relaxation and quasi-elastic neutron scattering (QNS). Combined NMR, INS and QNS studies have contributed to the understanding of rotational tunnelling and to the determination of the rotational potentials [5–8].

Various materials have been studied, and first of all rotational tunnelling was observed in methyl benzenes [2–4, 6, 9–13], methyl pyridines [5, 14, 15], and acetates [7, 16–20]. A large tunnel splitting was also found in tetramethyl lead by INS [21], and important quantum effects were detected by NMR for all the series compounds $X(CH_3)_4$, where X = Si, Ge, Sn and Pb [22].

These compounds provide an example of the influence of the increasing X–C bond length upon the barrier height. From X = Si to X = Pb the barrier height diminishes from about 6 to 0.6 kJ/mol and the tunnel splitting increases from less than 0.2 to 35 μeV or more. In the same succession the frequency and temperature dependences of the NMR relaxation rates T_1^{-1} change characteristically. We have therefore investigated the relaxation behaviour of all the compounds, and we have included methyllithium which has a similar structure. If necessary and possible, INS and QNS measurements have been made in addition, and the results of other workers which came to be known in the meantime, have also been considered, such as the NMR studies of Ligthelm [23, 24] on $Ge(CH_3)_4$ and the "field cycling" experiments of Takeda and Chihara on $Si(CH_3)_4$ [25] and of Gabrys on $Ge(CH_3)_4$ [26].

Reprint requests to Prof. Dr. W. Müller-Warmuth, Institut für Physikalische Chemie der Universität Münster, Schlossplatz 4/7, D-4400 Münster.

0340-4811 / 84 / 0100-0066 $ 01.3 0/0. – Please order a reprint rather than making your own copy.

In a preceding paper [8] INS and NMR data of $Sn(CH_3)_4$ have been explained in terms of the molecular and crystal structure which establishes the existence of two-types of non-equivalent methyl groups in the ratio 3 : 1. The crystal structure of the other tetramethyls is not known, but non-equivalent methyl rotors may exist as well. $LiCH_3$ consists of quaternary units, where four lithium atoms form a tetrahedron with the methyl groups situated opposite to the four surfaces of the Li tetrahedron [27]. The separation between methyl groups (r_{CC} = 3.69 Å) is comparable with those of $Pb(CH_3)_4$.

2. Theory

2.1. The CH_3 rotator

The energy levels of the one-dimensional methyl rotator are given by the eigenvalues of the Schrödinger equation

$$-B\frac{\partial^2\Psi}{\partial\Phi^2}+V(\Phi)\,\Psi=E\,\Psi\,, \tag{1}$$

where $B=\hbar^2/2\,I=0.6475$ meV $=0.0625$ kJ/mol is the rotational constant with I being the momentum of inertia. The rotational potential $V(\Phi)$ is generally described by a Fourier expansion with the basic threefold symmetry (C_3) of the methyl groups and tabulated eigenvalues are available [28] for potentials

$$V(\Phi)=\frac{V_3}{2}[1+(-1)^k\cos 3\,\Phi]+\frac{V_6}{2}[1+(-1)^k\cos 6\,\Phi]\,. \tag{2}$$

k characterizes the relative phase meaning either no shift between the three- and sixfold terms ($k=0$) or a phase shift of $\pi/2$ ($k=1$).

According to the C_3 symmetry of the methyl group three types of rotator eigenstates can be distinguished which are labeled A^v, E_a^v and E_b^v with v being the index of the torsional state. The E states are degenerate. In a predominant threefold potential three such substates form the torsional system of the molecule. The rotational behaviour is quite different for different regions of temperature. At low temperature the methyl group is an oscillator which vibrates in a certain torsional state v about one of three equivalent orientations. The torsional states are split into two tunnelling states (A^v, E^v) owing to the overlap of the wave functions in adjacent wells of the potential.

$$\omega_t^v=(E^v_{(E_a,E_b)}-E^v_{(A)})/\hbar$$

is called the tunnelling frequency. Apart from tunnelling transitions, which involve a spin flip, phonon-induced transitions to the first excited level E^1 with energy separation E_{01} from the ground state become relevant with increasing temperature.

At elevated temperatures more excited torsional levels get involved and finally random reorientations over the barrier become important. As a characteristic of the potential, in this limit the activation energy E_A is used, which is the energy difference between the top of the barrier and E^0. For a given potential, Eq. (2), E_A may be calculated from the eigenvalues, or in the other way round, the potential may be derived, if E_A and/or ω_t^0 and/or E_{01} are known. ω_t, E_{01} and E_A as well as the correlation time τ_c for the reorientation may be determined by NMR, INS and QNS experiments.

2.2. Spin-lattice relaxation

The theory of the NMR spin-lattice relaxation of tunnelling methyl groups was first established by Haupt [29] and has been further developed in the meantime [5, 24, 30]. Spin-lattice relaxation and rotation or tunnelling, respectively, are coupled by the dipole-dipole interaction between the protons. Both the spatial and the spin coordinates are treated as quantum-mechanical operators, and only those combinations of the spatial and nuclear functions are possible which satisfy the Pauli exclusion principle, and which are invariant under a cyclical permutation of the coordinates. We have therefore an A spin state combined with the A rotator state with a total spin of 3/2, and E_a or E_b states with a total spin of 1/2 which combine with E_b or E_a, respectively. In an external field the A states are split into a quartet, the E_a and E_b states are doublets. Thus proton relaxation by spin flips at the Larmor frequency ω_0 or at $2\omega_0$ is always connected with a change of symmetry of the rotator state, either from A to E or from E_a to E_b.

The first case holds for the relaxation of an isolated methyl group, and here the relaxation rate is proportional to the spectral densities occurring at the frequencies $\omega_t\pm\omega_0$ and $\omega_t\pm 2\omega_0$. Intermolecular interactions between protons of different methyl groups or with other protons lead to the same type

of transitions and in addition to spectral densities at frequencies ω_0 and $2\omega_0$ since the E states of the rotator are degenerate. As a final result, the well-known classical BPP expression for a polycrystalline sample,

$$\frac{1}{T_1} = C\left[\frac{\tau_c}{1+\omega_0^2\tau_c^2} + \frac{4\tau_c}{1+4\omega_0^2\tau_c^2}\right] \tag{3}$$

has to be replaced by

$$\frac{1}{T_1} = C_{AE}\left[\frac{\tau_c}{1+(\omega_t+\omega_0)^2\tau_c^2} + \frac{\tau_c}{1+(\omega_t-\omega_0)^2\tau_c^2} + \frac{4\tau_c}{1+(\omega_t+2\omega_0)^2\tau_c^2} + \frac{4\tau_c}{1+(\omega_t-2\omega_0)^2\tau_c^2}\right] + C_{EE}\left[\frac{\tau_c}{1+\omega_0^2\tau_c^2} + \frac{4\tau_c}{1+4\omega_0^2\tau_c^2}\right]. \tag{4}$$

For the intra-methyl dipolar interaction C_{AE} is given by

$$C_{AE} = \frac{9}{10}\left(\frac{\mu_0}{4\pi}\right)^2 \frac{\gamma^4\hbar^2}{b^6} p\,\delta^2,$$

where p denotes the ratio of methyl protons over the total number of protons, and δ^2 is the effective relaxation efficiency factor [24, 29] which is slightly temperature dependent and less than one. Using $\mu_0/4\pi = 1\cdot10^{-7}$ SI units, $\gamma(^1H) = 2.675\cdot10^8\,T^{-1}s^{-1}$, $\hbar = 1.055\cdot10^{-34}$ Js, $b = 1.78\cdot10^{-10}$ m (proton-proton distance) it follows $(C_{AE}/(p\,\delta^2) = 4.0\cdot10^9\,s^{-2}$. For the inter-methyl contribution of course no estimate can be made.

In order to compare the results of experimental T_1^{-1} measurements with Eq. (4) a number of complications have to be observed:

- ω_t is temperature-dependent, and only at very low temperatures it equals ω_t^0, the tunnelling splitting ($A \leftrightarrow E$) in the torsional ground state. With increasing temperature ω_t decreases, and at elevated temperatures it tends toward zero. The reason is the dynamic mixing of tunnel splittings of various torsional states in combination with a coupling of the rotor system to the phonons [5, 19, 30–33]. The problem is not yet fully understood. Only recently Hewson [33] presented a somewhat more sophisticated model which takes into account the full density of states of the material. According to this work, the temperature dependence of the shifting should increase more slowly than the exponential $\exp(-E_{01}/RT)$. This seems to be consistent with experimental observations [8, 34].
- For the relation between the correlation time τ_c of the motion and the temperature no simple Arrhenius law can be assumed, since the apparent activation energy decreases for decreasing temperature. The temperature dependence of τ_c^{-1} is approximated by [5, 6, 8]

$$\frac{1}{\tau_c} = \frac{1}{\tau_0'}\exp(-E_A'/RT) + \frac{1}{\tau_0''}\exp(-E_A''/RT). \tag{5}$$

  Limiting values are: $E_A' = E_A$ in the high temperature region, if only rotational states in the neighbourhood of the top of the potential contribute to τ_c^{-1}; and $E_A'' = E_{01}$ at low temperatures, when only the groundstate is populated. A more detailed analysis is given by Ligthelm [24].
- For methyl groups the relaxation has to be interpreted by the "Symmetry Restricted Spin Diffusion" (SRSD) model of Emid and Wind [30, 35]. The process of the establishment of a common (Zeeman) spin temperature has to be described by couplings of the Zeeman-, dipolar-, tunnelling- and rotational polarization subsystems with one another and with the lattice, and therefore the spin-lattice relaxation appears to be multi-exponential. Here the tunnelling system accounts for the population difference between A and E_a, E_b species, and the rotational polarization for the population difference between E_a and E_b, respectively.

For the interpretation and discussion of the NMR spin-lattice relaxation data of this paper the following limiting cases of (4) are of importance:

a) $\omega_t \ll \omega_0$ or $\omega_t\tau_c \ll 1$.

Equation (4) reduces to the classical Eq. (3), and $C = 2C_{AE} + C_{EE}$.

b) $\omega_t \gg \omega_0$.

Equation (4) leads to

$$\frac{1}{T_1} = 4C_{AE}\frac{\tau_c}{1+\omega_t^2\tau_c^2} + C_{EE}\left[\frac{\tau_c}{1+\omega_0^2\tau_c^2} + \frac{4\tau_c}{1+4\omega_0^2\tau_c^2}\right] \tag{6}$$

and in the $\ln(1/T_1)$ vs. $1/T$ representation two maxima occur, one for $\omega_0\tau_c = 0.62$ as in case a), the other one for $\omega_t\tau_c = 1$.

c) $\omega_t = \omega_0$, $2\omega_0$ and $\omega_0 \tau_c \gg 1$.

Due to the denominators of the respective terms of (4) additional peaks ("tunnelling assisted maxima") occur in the $\ln(1/T_1)$ vs. $1/T$ plot at those temperatures where these conditions are fulfilled.

d) $\omega_t \approx \omega_0$.

If ω_t is of the order of ω_0, maxima occur at $(\omega_t \pm \omega_0)\,\tau_c \approx 1$ and $(\omega_t \pm 2\omega_0)\,\tau_c \approx 1$ which may not be easily distinguished from those for $\omega_t \tau_c = 1$ and $\omega_0 \tau_c = 0.62$ since they are all located in a similar temperature range.

2.3. Relaxation in the rotating frame

For some cases we have applied the method of relaxation measurements in the rotating frame. The "classical" formula [36],

$$\frac{1}{T_{1\varrho}} = C\left[\frac{5}{2}\frac{\tau_c}{1+\omega_0^2\tau_c^2} + \frac{\tau_c}{1+4\omega_0^2\tau_c^2} + \frac{3}{2}\frac{\tau_c}{1+4\omega_1^2\tau_c^2}\right] \tag{7}$$

which replaces (3) for this situation, of course has also to be modified in order to account for tunnelling. As a consequence, there will occur maxima of $1/T_{1\varrho}$ at temperatures where $2\omega_1 \tau_c \approx 1$ and $\omega_t \tau_c = 1$ (if $\omega_t \gg \omega_1$), and the behaviour near $\omega_0 \tau_c = 1$ is influenced by ω_t too.

2.4. Neutron scattering

The theory of neutron scattering from a one-dimensional tunnelling rotator has been developed by several authors [1, 17, 37]. More details are given in the preceding paper [8]. Transitions within the various rotational levels of the methyl group can directly be observed by inelastic neutron scattering (INS). In particular, the tunnel splitting of the torsional ground state can be measured using high resolution instruments, and the torsional splittings with standard time of flight or three axis spectrometers.

Furthermore, scattering from a reorienting methyl group leads to a quasielastic line with width Γ_{qu} centered at zero energy transfer. From this quasielastic scattering (QNS) the barrier height E_A of the rotational potential can be extracted. A special method for investigating quasielastic scattering is the so-called "fixed-window-method" [1] employed also in the present study. The elastic intensity I_{el} is measured in an energy window of the width of the instrumental resolution Γ_{res} as a function of temperature. At that temperature where Γ_{qu} becomes of the order of magnitude of Γ_{res}, there is a loss of intensity from the energy window and a step in the $I_{el}(T)$ curve is produced. For a one-dimensional threefold rotation

$$\Gamma_{qu} = \frac{3\hbar}{2\tau_c'} = \Gamma_0 \exp(-E_A'/RT)$$

holds with τ_c' being the high temperature approximation of (5) Half intensity is lost at a temperature $T_{1/2}$ where $\Gamma_{qu} = \Gamma_{res}$ or

$$E_A' = \ln\left(\frac{\Gamma_0}{\Gamma_{res}}\right) T_{1/2}\,. \tag{8}$$

3. Experimental Details and Results

3.1. Sample preparation and apparatus

The materials were purchased from Ventron and Merck companies, respectively. The tetramethyl compounds are all liquid at room temperature. They were further cleaned by distillation and oxygen was removed by several freeze-pump-thaw cycles. The samples were sealed in glass ampoules. In order to obtain really crystalline materials, before measuring the samples were first cooled down to a temperature of approximately 50 K below the melting point, then warmed up and tempered at 5 K below the melting point for several hours. Methyl lithium was obtained as a solution in ether, and it was isolated by evaporation of the solvent. It was then dried for one day at 80 °C and sealed under inert gas. The crystal structure of $Sn(CH_3)_4$ was determined [38], that of $LiCH_3$ is known [27].

The NMR experiments were performed using a Bruker SXP pulsed spectrometer at two different Larmor frequencies $\omega_0/2\pi = 15$ MHz and 30 MHz, and over a temperature range from 5 K to the melting point. A home-made probe was inserted into a continuous flow liquid helium cryostat from Oxford Instruments. The temperature was controlled by a commercial system and independently measured by Ni-Cr/Au-Fe thermocouples. Temperatures below 20 K were measured in addition by the resistivity of a germanium semiconductor. The accuracy was better than ± 0.5 K over the whole range.

Table 1. Numerical values of the apparent activation energies E'_A and E''_A, the limiting correlation times τ'_0 and τ''_0, and C, C_{AE}, C_{EE} as derived from the experimental curves; a value in bracket means: not immediately derived, but estimated. The tunnelling energies $\hbar\omega_t$ are determined at the very temperature indicated in brackets.

	E'_A kJ/mol	E''_A kJ/mol	τ'_0 10^{-12} s	τ''_0 10^{-11} s	C 10^9 s^{-2}	C_{AE} 10^9 s^{-2}	C_{EE} 10^9 s^{-2}	$\hbar\omega_t(T)$ μeV
γ-$Si(CH_3)_4$	6.5	4.7	0.53	0.91	5.7	(2.7)	0.3	0.12 (45) 0.062 (52) 0.046 (71) 0.026 (67)
$Ge(CH_3)_4$	5.2	4.2	0.35	0.16	6.2	(3.0)	0.3	0.12 (52) 0.25 (46)
$Sn(CH_3)_4$	1.9 3.4	1.1 (1.8)	0.40 (0.06)	2.5 1.5	(5.5)	2.5 (2.5)	0.49 0.17	4.6 (38) 0.7 (40)
$Pb(CH_3)_4$	0.62	0.23	11	125	(2.2)	0.98	0.20	2.6 (29) 20 (100)
$LiCH_3$	4.5	2.8	1.3	3.6	4.7			0.12 (35)

All relaxation measurements were carried out applying $90° - \tau - 90°$ pulse sequences. According to the SRSD model outlined in Sect. 2.2, $1/T_1$ can be determined from the initial slope of the plot $\ln(M_0 - M_z)/M_0$ as a function of time. Since the relaxation curves were non-exponential in most cases, the error of the experimental relaxation rates may be typically 15–20% though the absolute measuring error is much smaller on the average. $T_{1\varrho}$ measurements were performed in the usual way by a sequence consisting of a 90° pulse in the y-direction, which brings the nuclear magnetization into the x-direction, and a pulse of amplitude $H_1 = \omega_1/\gamma$ of long duration t_1 applied along the x-direction. The amplitude of the free induction decay is then observed as a function of t_1. The $T_{1\varrho}$ relaxation curves are also multi-exponential in agreement with the SRSD model.

The neutron scattering experiments were carried out using a high resolution backscattering and a thermal time of flight spectrometer at the research reactor DIDO in Jülich. The experimental procedure is as described in [8].

3.2. Summary of data

In order to facilitate the presentation of the experimental results for the various materials and their discussion in part 4, all the parameters which were derived from the NMR relaxation data are listed in Table 1. From time to time we will refer to this table. In a second table, Table 2, the parameters derived from INS and QNS are presented together with available literature data.

Table 2. Tunnel splittings $\hbar\omega_t^0$ in the ground state, torsional excitations E_{01} from the ground state and activation energies E_A measured by neutron scattering (INS, QNS), infrared spectroscopy (IR), thermodynamic studies (CAL) and high temperature NMR of other workers. Data which are not obtained within the present study are indicated by [a] modified results from [25]; [b] [21]; [c] C. I. Ratcliffe and T. C. Waddington, J. Chem. Soc. (Faraday Transact. 2) **72,** 1840 (1976); [d] [40]; [e] J. R. Durig, S. M. Craven, and J. Bragin, J. Chem. Phys. **52,** 2046 (1969); [f] M. Harada, T. Atake, and H. Chihara, J. Chem. Thermodyn. **9,** 523 (1977); [g] D. W. Scott et al., J. Phys. Chem. **65,** 1320 (1961); [h] A.-J. Valerga and J. E. Kilpatrick, J. Chem. Phys. **52,** 4545 (1970); [i] [41]; [j] [42]; [k] T. Hasebe, G. Soda, and H. Chihara, Proc. Japan Acad. **51,** 168 (1975); [l] [24].

	$\hbar\omega_t^0$ μeV	E_{01}/kJ/mol		E_A/kJ/mol		
		INS	IR	QNS	CAL	HT NMR
γ-$Si(CH_3)_4$	0.21[a]	1.91[c]	1.96[e]	7.4	6.5[f]	6.6[i] 6.6[j]
	0.13[a]	2.12[c]	2.13[e]		6.7[g]	6.8[k]
$Ge(CH_3)_4$	0.47	1.69[c,d]	1.61[e]		3.1[h]	2.7[i] 5.2[l]
$Sn(CH_3)_4$	13.3 1.72	1.27 1.71	1.22[e]	3.4[d]		1.9[i] 2.6[k]
$Pb(CH_3)_4$	35[b]	0.3		0.7		0.75[i]
$LiCH_3$	0.3	–		5.4		

3.3. Tetramethylsilane

$Si(CH_3)_4$ exists in three different modifications [39]. We have studied the stable γ-phase and the metastable β-phase. Figs. 1 and 2 show the relaxation rates plotted against the inverse of the temperature. On the whole, at least Fig. 1 looks similar as the curve generally observed for relaxation, where

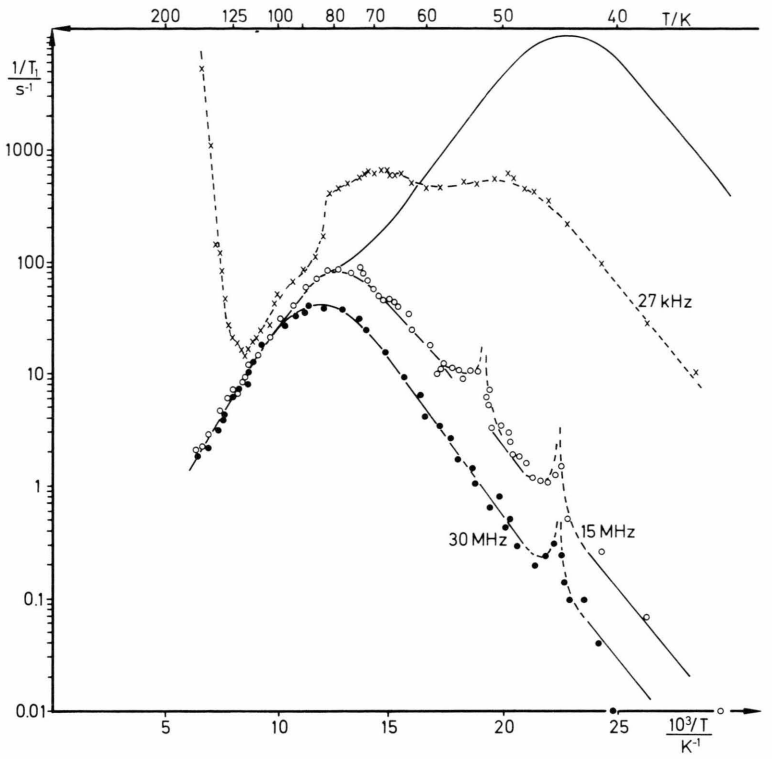

Fig. 1. Proton spin-lattice relaxation rate $1/T_1$ and relaxation rate in the rotating frame $1/T_{1\varrho}$ versus reciprocal temperature for γ-$Si(CH_3)_4$. The solid lines indicate the "classical" behavior of the CH_3 rotator, Eqs. (3) and (7), the dotted lines serve as guide to the eye.

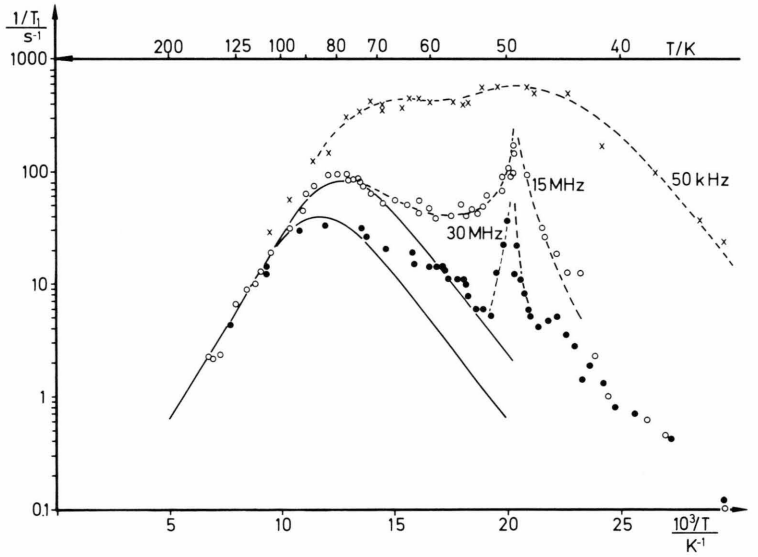

Fig. 2. Same as Fig. 1 for β-$Si(CH_3)_4$.

tunnelling does not play a role. Inspection of Fig. 2 shows that this curve looks more anomalous than that of Fig. 1 because somewhat larger tunnelling frequencies make the T_1^{-1} dependences deviate more strongly from the classical behaviour. For both curves the frequency dependent maxima are located in the temperature range 75–85 K, and the maxima of $T_{1\varrho}^{-1}$ corresponding to $2\omega_1\tau_c = 1$ occur between 45 and 50 K. But there are some remarkable features in addition.

First of all tunnelling-assisted maxima are observed, in the case of γ-$Si(CH_3)_4$ for $\omega_0/2\pi =$

30 MHz and for $\omega_0/2\pi = 15$ MHz at the same temperature of 44.6 K, and for 15 MHz in addition at 52 K. An analoguous maximum for β-$Si(CH_3)_4$ occurs at 49.5 K. Strongly non-exponential relaxation at these maxima agrees with the SRSD theory, but cause a greater uncertainity of the values. From the resonance conditions of Sect. 2.2 and a proper combination of the experimental results the tunnelling frequencies at the respective temperatures are obtained. The maxima of $T_{1\varrho}^{-1}$ near 65–70 K correspond to the condition $\omega_t \tau_c = 1$.

For both phases a fixed-window scan at the backscattering spectrometer with $\Gamma_{res} = 0.4\,\mu$eV has been performed. Using a Γ_0 corresponding to $\tau_0 = 10^{-12}$ s an activation energy $E'_A = 7$ kJ/mol can be estimated from (8) for β-$Si(CH_3)_4$. The value for the γ phase is somewhat larger, in agreement with the NMR results. Both values, however, exceed those derived from the high temperature NMR-T_1.

3.4. Tetramethylgermanium

The experimental T_1^{-1} results from $Ge(CH_3)_4$ as shown in Fig. 3 are reminiscent of those from $Si(CH_3)_4$ of Fig. 2, but there is still more deviation from the classical behavior at the low temperature side. Tunnelling-assisted maxima occur for 30 MHz at temperatures of 45.9 K and 51.8 K, which is quite close to the classical $1/T_1$ maxima. At 15 MHz, tunnelling-assisted maxima are expected to occur even nearer to the maximum and thus they are even more strongly suppressed, since the condition $\omega_0 \tau_c \gg 1$ is not fulfilled. As a result, all the maxima appear to be significantly broadened.

The dependence of $T_{1\varrho}^{-1}$ on the reciprocal temperature is distinguished by a shoulder for $\omega_t \tau_c = 1$ near 54 K, by the influence of several terms that contain $(\omega_t \pm \omega_0)\,\tau$ and $(\omega_t \pm 2\omega_0)\,\tau$ in the denominator near 46 K, and by the maximum at 32 K which corresponds to $2\omega_1 \tau = 1$.

The density of states (DOS) of $Ge(CH_3)_4$ was already measured by Steenbergen and de Graaf [40], who assigned the line at 17.5 meV as belonging to the torsional excitation E_{01} of the methyl group.

We have completed the INS study by looking for possible tunnel splittings using high energy resolution. The spectrum is shown in Figure 4. The solid line is a fit which employs a scattering law containing an elastic line and two symmetric inelastic lines to account for tunnelling, the whole convoluted with

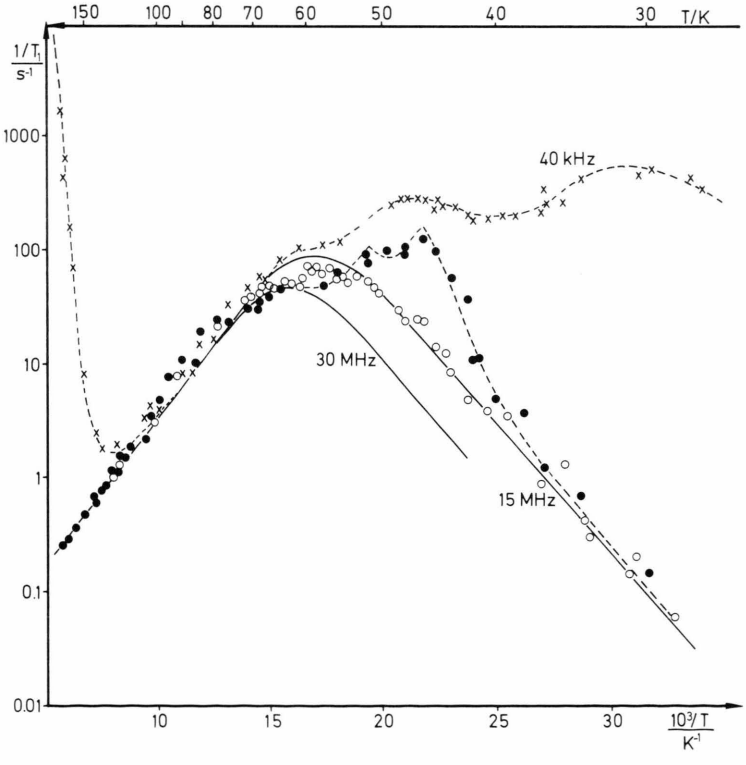

Fig. 3. Same as Fig. 1 for $Ge(CH_3)_4$.

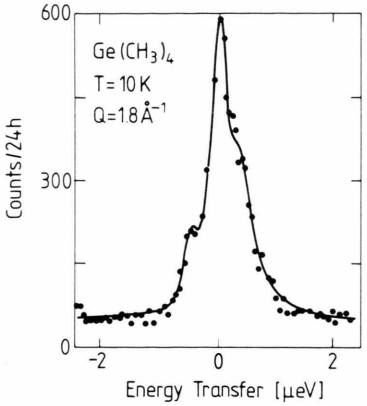

Fig. 4. High-resolution INS spectrum of $Ge(CH_3)_4$.

the asymmetric instrumental resolution. Thus a tunnelling energy $\hbar\,\omega_t^0 = 0.47\ \mu$eV is found. The intensity of this shows that the major part of all CH_3 groups is involved in this transition.

3.5. Tetramethyltin

Various INS and NMR results were already reported in the preceding paper [8]. The temperature dependence of the spin-lattice relaxation rate looks very similar to that of earlier experiments [5, 6] and that of tetramethyllead shown in Fig. 5 which are characteristic of large tunnel splittings, $\omega_t^0 \gg \omega_0$. INS tunnelling experiments and a subsequent structure analysis revealed the existence of two inequivalent types of methyl groups. We shall profit from these results in the discussion.

3.6. Tetramethyllead

Figure 5 shows the temperature dependence of $1/T_1$. The maxima occur at rather low temperatures and the curves look similar to those often observed [5, 6] for $\omega_t \gg \omega_0$. The tunnel splitting was determined earlier by Alefeld and Kollmar [21] and amounts to 35 μeV. We have tried to measure in addition the energy separation between the torsional first excited and ground states by INS and observed a weak and rather broad peak at $T = 15$ K with an energy transfer of 0.30 kJ/mol.

3.7. Methyllithium

The temperature dependence of T_1^{-1} (Fig. 6) looks rather classical, but is distinguished by a small frequency-dependent additional maximum at high temperatures and by a bending of the curves at low

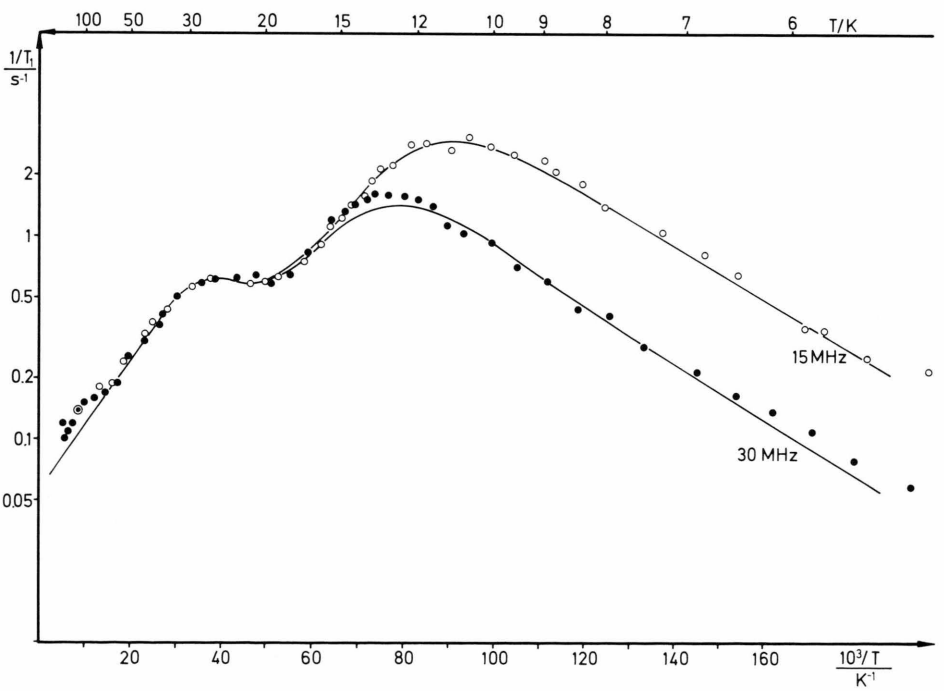

Fig. 5. Proton spin-lattice relaxation rate versus reciprocal temperature for $Pb(CH_3)_4$. The solid line corresponds to the fit discussed in the text using Eqs. (5) and (6).

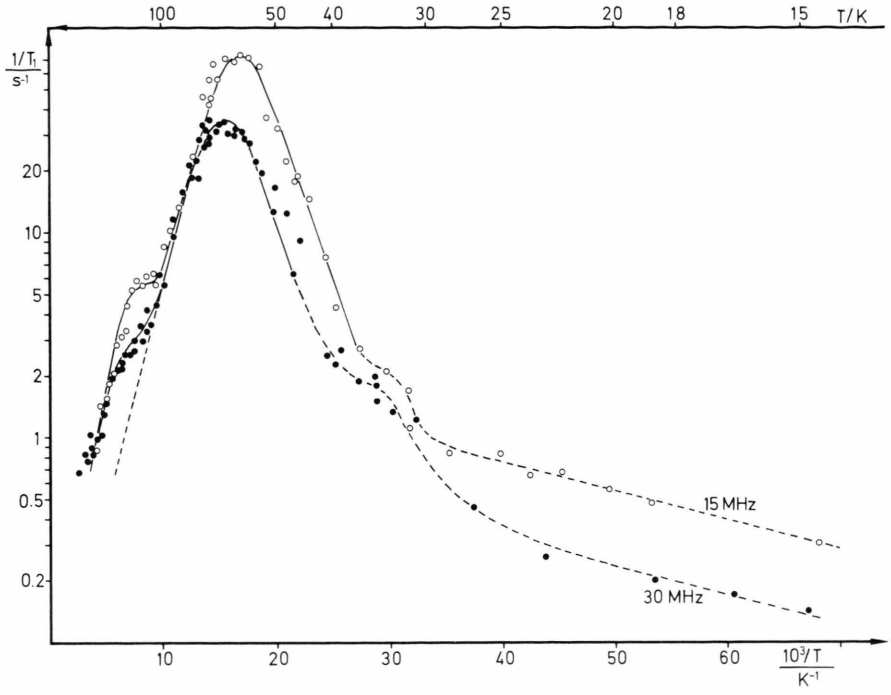

Fig. 6. Proton spin-lattice relaxation rate versus reciprocal temperature for $LiCH_3$. The solid lines indicate "classical behaviour" (Eq. (3)), the dotted lines serve as guide to the eye.

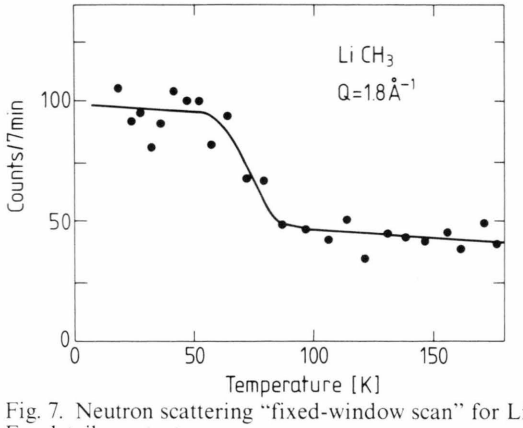

Fig. 7. Neutron scattering "fixed-window scan" for $LiCH_3$. For details see text.

temperatures. Weak tunnelling-assisted maxima can be recognized near $T = 35$ K. At this temperature, $\omega_t/2\pi = 30$ MHz.

A neutron fixed-window scan (Fig. 7) shows a step with $T_{1/2} = 71$ K. The evaluation according to (8) leads to $E'_A = 5.4$ kJ/mol using $\tau_0 = 10^{-12}$ s. The low temperature high resolution spectrum shows a small broadening compared to the instrumental resolution. On the assumption that all methyl groups are equivalent and contribute to the unresolved tunnelling lines, a tunnel splitting $\hbar\omega_t^0 = 0.3 \pm 0.1$ μeV can be estimated. The DOS shows an unstructured intensity up to rather high energy transfer.

4. Interpretation and Discussion

4.1. Tetramethylsilane and tetramethylgermanium

The temperature dependences of $1/T_1$ deviate in the succession γ-$Si(CH_3)_4$, β-$Si(CH_3)_4$, $Ge(CH_3)_4$ more and more from the classical behaviour of (3). The points of Fig. 1 may still be described by (3) and (5) using the parameters of Table 1 (solid lines). Characteristic features are, however, small tunnelling-assisted maxima on the right hand side of the curves.

The $1/T_1$ data of Figs. 2 and 3, on the other hand, can no longer be discussed in terms of (3), but (4) has to be applied in the low temperature region. This means, that, apart from the tunnelling-assisted maxima, the various maxima of the individual terms of (4) near $(\omega_t \pm \omega_0)\tau_c = 1$ and $(\omega_t \pm 2\omega_0)\tau_c = 1$ smear the curves on the low temperature side of the frequency dependent maxima. This typical appearance is due to the particular temperature de-

pendence of ω_t which makes (3) again valid at sufficiently high temperatures. We did not attempt to describe $1/T_1$ quantitatively; we only determined the temperature dependences of the correlation time, (5), and the associated parameters, Table 1. The solid lines of Figs. 1 to 3 indicate the classical limit of (3).

The sudden and rapid increase of $1/T_{1\varrho}$ at high temperatures above 120 K and 130 K (Figs. 1 and 3), respectively, indicates the onset of the rather slow rotational motion of the whole molecules. The corresponding activation energies are 37 ± 2 kJ/mol for γ-$Si(CH_3)_4$ and 43 ± 4 kJ/mol for $Ge(CH_3)_4$. From linewidth measurements Smith derived values of 29 and 42 kJ/mol, respectively [41], and Albert and Ripmeester found 36 kJ/mol [42] for $Si(CH_3)_4$.

Apart from this, $T_{1\varrho}^{-1}$ is governed by the relation $\omega_t \gg \omega_1$. The upper solid line of Fig. 1 shows the temperature dependence of $T_{1\varrho}^{-1}$ owing to (7). The influence of tunnelling changes this "classical" behaviour greatly. The maximum on the right hand side occurring near $2\omega_1 \tau_c \approx 1$ at 50 K is no longer governed by the relaxation strength C, but finally by C_{EE}, which is much smaller since it accounts only for intermethyl interactions. In the same time the intramethyl interactions produce maxima near 65 and 70 K occurring at $\omega_t \tau_c = 1$ and governed by C_{AE}. We did not attempt to calculate the temperature dependence in detail, because there is a continuous transition from the classical to the quantum-mechanical behaviour of the CH_3 rotation as the temperature is decreased, and because there is in addition the importance of terms at frequencies $\omega_t \pm \omega_0$ and $\omega_t \pm 2\omega_0$, similar to those appearing in (4). From the height of the $(2\omega_1 \tau_c = 1)$-maximum it is possible to make an estimate of C_{EE} which is also given in Table 1. Figure 2 shows a similar dependence of $T_{1\varrho}^{-1}$ for β-$Si(CH_3)_4$, whereas for $Ge(CH_3)_4$ (Fig. 3) the tunnelling-assisted maxima near $\omega_t = \omega_0$ and $\omega_t = 2\omega_0$ seem to have effect on $T_{1\varrho}$ too, since $T_{1\varrho}$ is measured at the Lamor frequency ω_0. The $T_{1\varrho}^{-1}$ maxima for $\omega_t \tau_c = 1$ and $2\omega_1 \tau_c = 1$ occur near 18 K and 30 K, respectively.

Using the various results we are able to determine the temperature dependence of the tunnelling frequency (Figs. 8 and 9). In order to explain the procedure, the case of $Ge(CH_3)_4$ (Fig. 9) is discussed first, since for this case ω_t^0 has directly been measured by INS at $T = 10$ K (full circle). The other full circles are the points extracted from Fig. 3 for the respective resonance conditions. Further data are available from studies of Ligthelm [24] and Pintar [43]. There is finally the result of Gabrys [26] who used a field-cycling technique to detect a tunnel resonance at $\omega_t/2\pi = 58$ MHz. She interpreted her result as belonging to the resonance condition $\omega_t = 2\omega_0$.

In the same way Fig. 8 is obtained for γ-$Si(CH_3)_4$. Proper assignment of our results is only possible by a re-interpretation of the field-cycling results of Takeda and Chihara [25]. These authors report tunnelling frequencies $\omega_t^0/2\pi = 15.8$ and 24.0 MHz. We believe that these values belong to $\omega_t = 2\omega_0$ as

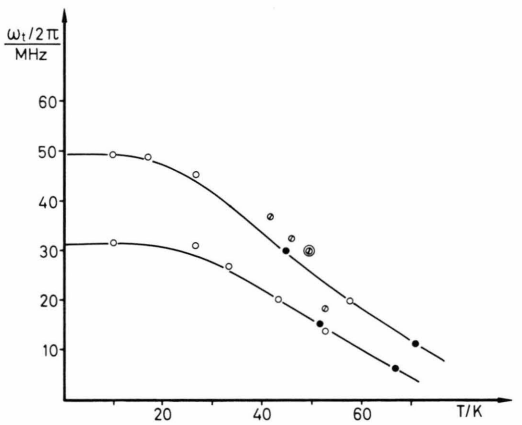

Fig. 8. Temperature dependence of the tunnelling frequencies of γ-$Si(CH_3)_4$ as derived from this work (●) and from a re-interpretation of the data [25] (○). The points ⌀ correspond to β-$Si(CH_3)_4$ either from this work (⌀) or from [24].

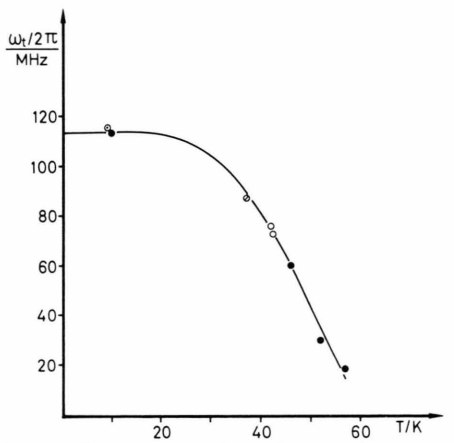

Fig. 9. Temperature dependence of the tunnelling frequency of $Ge(CH_3)_4$, this work: ●, [24]: ○, [26]: ⊙, [43]: ⌀.

in the case of $Ge(CH_3)_4$, and from their measurements we extracted the data which are plotted in Fig. 8 together with our own results. There is consistency between all the data. Two different tunnelling frequencies and their temperature dependences have been found. For β-$Si(CH_3)_4$ insufficient data are available. But it is clear from the few points of Fig. 8 that the tunnelling frequencies must be slightly higher than those for γ-$Si(CH_3)_4$. Ligthelm made also some measurements [24], but he did not indicate the particular phase. Comparison shows that he must have studied β-$Si(CH_3)_4$.

Examination of Figs. 8 and 9 yields an exponential temperature dependence for the shift of the tunnelling frequency

$$\Delta\omega_t \equiv \omega_t^0 - \omega_t(T) = \tilde{\omega}_0 \exp\{-E_S/RT\}$$

with $E_S = 0.66$ kJ/mol and 0.80 kJ/mol, respectively, for $Si(CH_3)_4$, and $E_S = 1.2$ kJ/mol for $Ge(CH_3)_4$. In agreement with the corresponding data for $Sn(CH_3)_4$ [8], E_S turns out to be smaller than E_{01} (Table 2) as expected by Hewson [33].

4.2. Methyllithium

Similar to the situation in the preceding section the limiting cases a), d) and c) of (4) apply also to $LiCH_3$ as the temperature is decreased. The solid lines of Fig. 6 correspond to Eqs. (3) and (5) and the parameters listed in Table 1. The additional maximum at $T = 143$ K accounts for a classical motion with relaxation strength $C = 2.5 \cdot 10^8\ s^{-2}$ and activation energy 6.5 kJ/mol. There is no conclusive explanation whether a small fraction of the methyl protons is responsible and whether the motion is rotation too. Although the sample was carefully prepared, impurities cannot completely be excluded. The larger activation energy derived from the QNS experiment may also originate in the additional process.

It is rather probable that, similar to $Si(CH_3)_4$ and $Ge(CH_3)_4$, the apparent low temperature activation energy E_A'' does not yet reflect E_{01} as the limiting value. In the temperature range considered, more states are still populated than the torsional ground state. The tunnelling frequency of 30 MHz obtained from the tunnelling-assisted maxima at $T = 35$ K agrees well with the groundstate splitting $\omega_t^0/2\pi = 77$ MHz estimated from INS. The data are, however, not sufficient in order to derive the temperature dependence of ω_t in detail.

4.3. Tetramethyltin and Tetramethyllead

Unlike the materials considered in the preceding two sections, the proton relaxation behaviour of both $Sn(CH_3)_4$ and $Pb(CH_3)_4$ can be described by (6) which holds for $\omega_t \gg \omega_0$. The $\ln(1/T_1)$ versus $1/T$ plot is then governed by two maxima, and the limiting value of $E_A'' = E_{01}$ is generally reached. The various parameters which fit the measured data are again listed in Table 1. In the case of $Sn(CH_3)_4$ there is the additional complication of non-equivalent methyl groups, which was already discussed in detail in the preceding paper [8]. Table 1 gives the parameters for both types of CH_3 groups. If the NMR-T_1 curve would be interpreted in terms of one type of CH_3 only, rather important changes in the parameters and inconsistencies with the INS results occur. Similar complications may be the reason for several problems arising from the interpretation of the results for $Pb(CH_3)_4$.

$Pb(CH_3)_4$ is distinguished by a rather low barrier to methyl rotation. Apparent activation energies E_A of a similar magnitude were only observed for 4-methylpyridine [15] and lithium acetate [16] so far, whose tunnel splittings – 517 μeV [14] and 250 μeV [17], respectively – are much greater. This agrees with our finding that the tunnel splitting of 35 μeV [21] does not go well together with the NMR data of tetramethyllead. Possibly, there are again two types of non-equivalent methyl groups. The more abundant CH_3 (1) groups then could govern the $1/T_1$ behaviour, and their tunnelling frequency must be much greater. On this assumption the measured splitting of 35 μeV may belong to the less abundant and more hindered methyl groups CH_3 (2). The small maximum of $1/T_1$ near 100 K then may be associated with the condition $\omega_t \tau_c = 1$ for CH_3 (2), and the larger maximum near 27 K with that for CH_3 (1). Further experiments are needed before a final conclusive answer can be given. Such experiments are in preparation.

At the present state of affairs we may establish that the measured values E_A' and E_A'' (Table 1) can apparently no longer be identified with the energy differences between the top of the barrier and the ground state, or between the two lowest lying torsional levels, respectively. In this region of transition energies, the CH_3 rotator resembles that of the free rotor with energies $E \sim m^2$ ($m = 0, 1, 2, 3, \ldots$). The grouping of torsional levels with tunnel split-

tings may become meaningless in this regime, and the theory of NMR relaxation by rotational tunnelling has to be reconsidered. The energy E_A'' which is determined from the relaxation rate at low temperature, between 5 and 10 K, and as well the energy of the weak and rather broad INS peak, may correspond to $m = 0, 1 \rightarrow 2$ transitions, since these are the only ones excited in this range. Furthermore, if the temperature increases to the range between 30 and 65 K, where E_A' was determined, transitions to the $m = 3$ and 4 state may also become involved. Assuming a preferentially three-fold potential, according to (1) with $V_3 = 0.2$ kJ/mol we obtain $E\,(m = 0 \rightarrow 2) = 0.29$ kJ/mol, $E\,(1 \rightarrow 2) = 0.23$ kJ/mol $E\,(0 \rightarrow 3) = 0.58$ kJ/mol and $E\,(0 \rightarrow 4) = 0.61$ kJ/mol. These values are close to those of Table 1, and the tunnel splitting should be of the order of 500 μeV.

5. Conclusions

Considering the ^1H NMR spin-lattice relaxation of the series compounds $X(CH_3)_4$ there is a continuous transition from a nearly classical behaviour for X = γ-Si to the typical case of tunnelling-induced relaxation for X = Sn; and X = Pb seems to approach already the free rotator. With this series we have an excellent example for studying the NMR-T_1 over a range which covers thermally activated reorientation and quantum-mechanical motion as well, if one goes from large potential barriers and high temperatures to small barriers and low temperatures. The activation energies strongly decrease in this sequence and the tunnel splittings increase. Many special features have been observed in the particular temperature- and frequency-dependences of the respective T_1^{-1} rates. The $T_{1\varrho}$ rates show already great influences from tunnelling for X = Si because the condition $\omega_t \gg \omega_1$ is already fulfilled, and the transition from the classical to the quantum-mechanical regime changes the behaviour greatly.

The values of E_A' in Table 1, in general, characterize the activation energies E_A. There is satisfactory agreement with the values of Table 2, but it is not clear why the QNS data are up to 20% larger. Comparison of Tables 1 and 2 shows further that for $Si(CH_3)_4$, $Ge(CH_3)_4$ and $LiCH_3$, E_A'' does not reproduce the energy difference E_{01} as found in many other studies [5, 6, 8] where the tunnel splittings were larger. For the present materials, the low temperature side of the relaxation peak does neither occur at so low temperatures that only the torsional ground state is populated, nor is the temperature sufficiently high to excite transitions like in the classical regime, where $E_A'' = E_A'$. For $Sn(CH_3)_4$ and $Pb(CH_3)_4$, on the other hand, only ground states are populated in the respective temperature range, and tunnelling induced relaxation is connected with non-magnetic transitions to the next lowest lying states.

The various values of τ_0', τ_0'', and C (Table 1) have the same order of magnitude as those observed earlier for other materials and as to be expected theoretically. An exception is of course $Pb(CH_3)_4$ where the methyl rotation is little hindered. NMR values for ω_t (last column of Table 1) are only derived at special elevated temperatures, either from "tunnelling-assisted maxima" or from the $\omega_t \tau_c = 1$ maxima. They are always smaller than the tunnelling frequencies in the ground state (Table 2).

There is a systematic relation between the experimental tunnel splittings (Table 2) and the experimental activation energies (Table 1). For the purpose of comparison, the semilogarithmic plot of Fig. 10 also contains some experimental results of other materials from earlier measurements and from other authors. This plot may be useful to locate tunnel splittings of materials to be studied in the future. It shows that the potential hindering the methyl rotation in the $X(CH_3)_4$ compounds is not far from being purely three-fold. Most points are located between the dotted line for $k = 1$ and $V_3/(V_3 + V_6) = 0.67$ and the solid line for $V_6 = 0$.

Table 3. Calculated potentials ($V_S = V_3 + V_6$, $\delta = V_3/V_S$) and length of the X–C bond for the $X(CH_3)_4$ compounds: [a] W. F. Sheenan and V. Schomaker, J. Amer. Chem. Soc. **74,** 3956 (1954); [b] L. O. Brockway and H. O. Jenkins, J. Amer. Chem. Soc. **58,** 2036 (1936); [c] [38]; [d] C. Wong and V. Schomaker, J. Chem. Phys. **28,** 1007 (1958).

	V_S/kJ/mol	δ	r_{XC}/nm
γ-$Si(CH_3)_4$	6.8 ± 0.5 7.6 ± 0.7	0.95 0.95	0.189[a]
$Ge(CH_3)_4$	5.9 ± 0.4	0	0.198[b]
$Sn(CH_3)_4$	2.9 ± 0.2 4.7 ± 0.6	0.86 0.77	0.214[c] 0.211[c]
$Pb(CH_3)_4$	0.20 ± 0.05 (2.1)		0.220[d] 0.229[b]
$LiCH_3$	6.4 ± 0.8	0.86	

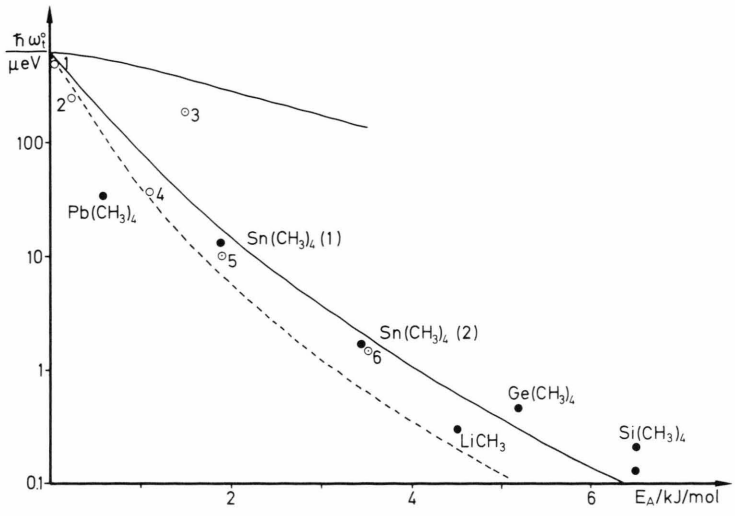

Fig. 10. Semilogarithmic plot of the measured tunnel splittings against experimental activation energies. In addition to the results of this work data are included for 1: 4-methylpyridine [14, 15]; 2: lithium acetate [16, 17]; 3: 2,6-dimethylpyridine [5]; 4: MDBP (4-methyl-2,6-ditertiarybutylphenol), [7, 9]; 5: 3-methylpyridine [5]; 6: 3,5-dimethylpyridine [5]. The solid line at the top is calculated for a purely sixfold potential, that in the center for a threefold potential, and the dotted line is a mixture with $k = 1$, $V_3/(V_3 + V_6) = 0.67$.

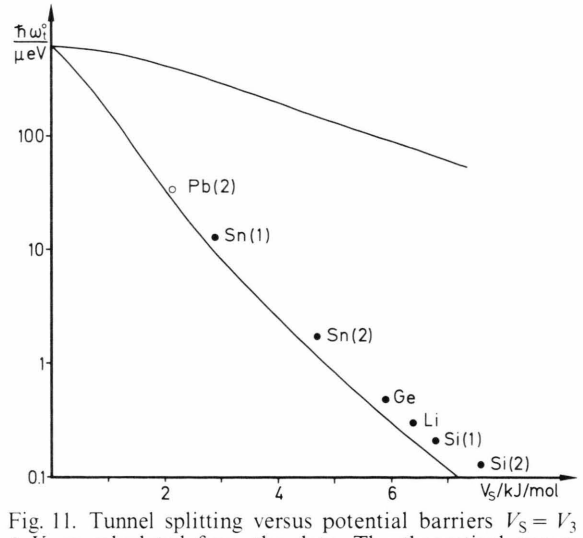

Fig. 11. Tunnel splitting versus potential barriers $V_S = V_3 + V_6$ as calculated from the data. The theoretical curves correspond to a purely sixfold and threefold potential function, respectively.

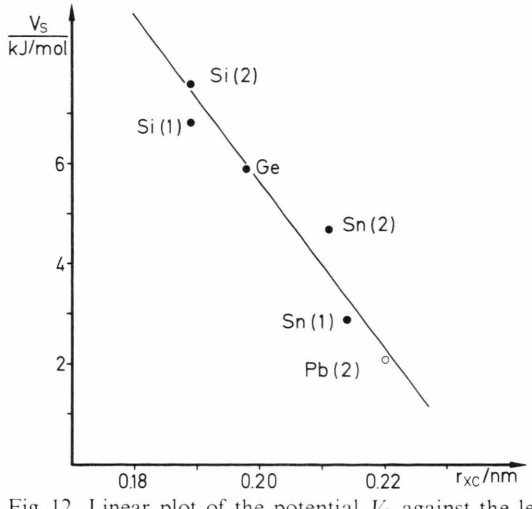

Fig. 12. Linear plot of the potential V_S against the length of the X–C bond.

This means that the potential function has some broadening connected with a dip at the top of the barrier. For reasons already discussed in Sect. 4.3, $Pb(CH_3)_4$ does not lie within the range which is covered by solutions of (1) with the potential (2). We may guess from the plot that the measured value of $h\,\omega_t^0(2)$ might be associated with an activation energy of about 1.5 kJ/mol, whereas $h\,\omega_t^0(1)$ has not yet been found.

Using the solutions of the Mathieu equation (1) we have calculated the potential functions (2) from the experimental values of ω_t^0, E_A and E_{01} (Tables 1 and 2). There are always two solutions. Ignoring the solutions which yield predominant sixfold potentials, the results of Table 3 have been obtained. In Fig. 11 they are plotted against the tunnel energies, which gives a reasonable relationship. Because of the error limits of the experimental data, or as in cases of $LiCH_4$ and $Pb(CH_3)_4$, because of missing information, the accuracy of the determination of $V_S = V_3 + V_6$ is not very high. But the result indicates clearly a similar potential shape for all com-

pounds. Table 3 also contains literature data for r_{CX}, the length of the X–C bond.

The potential barrier to methyl rotation is closely related to the molecular structure. This is demonstrated by Fig. 12 where V_S is plotted versus r_{CX}. Within the range studied we find a linear dependence on the X–C bond length (and as well on the C–C separation between different methyl groups of the same molecule) for the barrier,

$$V = V_0 (1 - r_{XC}/r_O)$$

with $V_O = 39$ kJ/mol and $r_O = 0.234$ nm. Realizing from Fig. 11 that the tunnel splitting can well be approximated by an exponential dependence on the potential, we obtain for the series compounds the approximation

$$h\,\omega_t^0 = A \exp(\alpha\, r_{XC})$$

with $A = 1.0 \cdot 10^{-15}\,\mu$eV and $\alpha = 172\ (\text{nm})^{-1}$. Therefore the potential is mainly of intramolecular origin and the methyl group reorientation is first of all hindered by neighbouring methyl groups of the same molecule.

[1] W. Press, Single Particle Rotation, Springer Tracts in Modern Physics, Vol. **92,** 1981.
[2] J. Haupt and W. Müller-Warmuth, Z. Naturforsch. **23 a,** 208 (1968).
[3] P. S. Allen and A. Cowking, J. Chem. Phys. **49,** 789 (1968).
[4] J. Haupt and W. Müller-Warmuth, Z. Naturforsch. **24 a,** 1066 (1969).
[5] W. Müller-Warmuth, R. Schüler, M. Prager, and A. Kollmar, J. Chem. Phys. **69,** 2382 (1978), and references given therein.
[6] W. Müller-Warmuth, R. Schüler, M. Prager, and A. Kollmar, J. Magn. Reson. **34,** 83 (1979).
[7] S. Clough, A. Heidemann, A.-J. Horsewill, J.-D. Lewis, and M. N. J. Paley, J. Phys. C **14,** L525 (1981), and references given therein.
[8] M. Prager, K.-H. Duprée, and W. Müller-Warmuth, Z. Phys. B.-Condensed, Matter **51,** 309 (1983).
[9] S. Clough and P. A. Beckmann, J. Phys. C **10,** L231 (1977).
[10] S. Clough and A. Heidemann, J. Phys. C **12,** 761 (1979).
[11] S. Takeda, G. Soda, and H. Chihara, Solid State Commun. **36,** 445 (1980).
[12] S. Clough, A. J. Horsewill, and A. Heidemann, Chem. Phys. Lett. **82,** 264 (1981).
[13] B. Gabrys and L. van Gerven, Chem. Phys. Lett. **82,** 260 (1981).
[14] B. Alefeld, A. Kollmar, and B. A. Dasannacharya, J. Chem. Phys. **63,** 4415 (1975).
[15] A. E. Zweers, H. B. Brom, and W. J. Huiskamp, Physica **85 B,** 239 (1977).
[16] P. S. Allen and P. Branson, J. Phys. C **11,** L121 (1978).
[17] S. Clough, A. Heidemann, and M. N. J. Paley, J. Phys. C **13,** 4009 (1980).
[18] S. Clough, A. Heidemann, M. N. J. Paley, and J. B. Suck, J. Phys. C **13,** 6599 (1980).
[19] S. Clough, A. Heidemann, and M. Paley, J. Phys. C **14,** 1001 (1981).
[20] F. Köksal, E. Rössler, and H. Sillescu, J. Phys. C **15,** 5821 (1982).
[21] B. Alefeld and A. Kollmar, Phys. Lett. **A 57,** 289 (1976).
[22] K.-H. Duprée, Diplomarbeit Münster 1977, unpublished.
[23] D. J. Ligthelm, R. A. Wind, and J. Smidt, Physica **100 B,** 175 (1980).
[24] D. J. Ligthelm, The Influence of the Spin-rotor Coupling of Methyl Groups in Solids and their NMR relaxation, Thesis, Delft 1981.
[25] S. Takeda and H. Chihara, J. Phys. Soc. Japan **51,** 642 (1982).
[26] B. Gabrys, Tunnelling of Methyl Groups in Solids Studied by NMR, Thesis, Leuven 1982.
[27] E. Weis and E. A. C. Sucken, J. ORGANOMET, Chem. **2,** 197 (1964).
[28] R. F. Gloden, Euratom Reports EUR 4349 and EUR 4358 (1970).
[29] J. Haupt, Z. Naturforsch. **26 a,** 1578 (1971).
[30] S. Emid and R. A. Wind, Chem. Phys. Lett. **33,** 269 (1975).
[31] P. S. Allen, J. Phys. C **7,** L 22 (1974).
[32] A. Hüller, Z. Physik **B 36,** 215 (1980).
[33] A. C. Hewson, J. Phys. C **15,** 3841 and 3855 (1982).
[34] S. Clough and A. Heidemann, J. Phys. C **12,** 761 (1979).
[35] S. Emid, R. J. Baarda, J. Smidt, and R. A. Wind, Physica **93 B,** 327 (1978).
[36] G. P. Jones, Phys. Rev. **148,** 332 (1966).
[37] A. Hüller, Phys. Rev. **B 16,** 1844 (1977).
[38] B. Krebs, G. Henkel, and M. Dartmann, Acta Cryst. in press.
[39] M. Harada, T. Atake, and H. Chihara, J. Chem. Thermodyn. **9,** 523 (1977).
[40] Chr. Steenbergen and L. A. de Graaf, Physica **96 B,** 15 (1979).
[41] G. W. Smith, J. Chem. Phys. **42,** 4229 (1965).
[42] S. Albert and J. A. Ripmeester, J. Chem. Phys. **57,** 2641 (1972).
[43] M. M. Pintar, 7th AMPERE International Summer School on Magnetic Resonance, Portoroz 1982.